


ORIGINAL ARTICLE

Let-7 mediated airway remodelling in chronic obstructive pulmonary disease via the regulation of IL-6

Tingting Di¹  | Yue Yang¹ | Congli Fu¹ | Zixiao Zhang¹ | Chu Qin¹ | Xiaoyan Sai¹ | Jiixin Liu¹ | Caixia Hu¹ | Mingfeng Zheng² | Yan Wu¹ | Tao Bian¹

¹Departments of Respiratory Medicine, Wuxi People's Hospital Affiliated to Nanjing Medical University, Wuxi, P.R. China

²Departments of Thoracic Surgery, Wuxi People's Hospital Affiliated to Nanjing Medical University, Wuxi, P.R. China

Correspondence

Tao Bian and Yan Wu, Departments of Respiratory Medicine, Wuxi People's Hospital Affiliated to Nanjing Medical University, Wuxi, Jiangsu, P.R. China. Emails: biantaophd@126.com; wuyanyangting@163.com

Funding information

The study was supported by the Natural Science Foundation of Wuxi [grant numbers JZYX01] and the project of Jiangsu Commission of Health [BJ17009]

Abstract

Background: Myofibroblast differentiation and extracellular matrix (ECM) deposition are observed in chronic obstructive pulmonary disease (COPD). However, the mechanisms of regulation of myofibroblast differentiation remain unclear.

Materials and methods: We detected let-7 levels in peripheral lung tissues, serum and primary bronchial epithelial cells of COPD patients and cigarette smoke (CS)-exposed mice. IL-6 mRNA was explored in lung tissues of COPD patients and CS-exposed mice. IL-6 protein was detected in cell supernatant from primary epithelial cells by ELISA. We confirmed the regulatory effect of let-7 on IL-6 by luciferase reporter assay. Western blotting assay was used to determine the expression of α -SMA, E-cadherin and collagen I. In vitro, cell study was performed to demonstrate the role of let-7 in myofibroblast differentiation and ECM deposition.

Results: Low expression of let-7 was observed in COPD patients, CS-exposed mice and CS extract (CSE)-treated human bronchial epithelial (HBE) cells. Increased IL-6 was found in COPD patients, CS-exposed mice and CSE-treated HBE cells. Let-7 targets and silences IL-6 protein coding genes through binding to 3' untranslated region (UTR) of IL-6. Normal or CSE-treated HBE cells were co-cultured with human embryonic lung fibroblasts (MRC-5 cells). Reduction of let-7 in HBE cells caused myofibroblast differentiation and ECM deposition, while increase of let-7 mimics decreased myofibroblast differentiation phenotype and ECM deposition.

Conclusion: We demonstrate that CS reduced let-7 expression in COPD and, further, identify let-7 as a regulator of myofibroblast differentiation through the regulation of IL-6, which has potential value for diagnosis and treatment of COPD.

KEYWORDS

airway remodelling, cigarette smoke, COPD, IL-6, let-7

Tingting Di and Yue Yang contributed equally to this work.

This is an open access article under the terms of the Creative Commons Attribution-NonCommercial-NoDerivs License, which permits use and distribution in any medium, provided the original work is properly cited, the use is non-commercial and no modifications or adaptations are made.

© 2020 The Authors. *European Journal of Clinical Investigation* published by John Wiley & Sons Ltd on behalf of Stichting European Society for Clinical Investigation Journal Foundation

1 | INTRODUCTION

COPD, a prevalent lung disease worldwide, is a chronic inflammatory airways disease.^{1,2} Airway remodelling, which constitutes the major pathological changes in COPD, can lead to pulmonary function decline, irreversible airflow limitation and airway obstruction. Myofibroblast differentiation, one of the primary molecular mechanisms of airway remodelling in COPD, is characterized by the production of ECM, expression of α -smooth muscle actin and an enhanced capacity to migrate.³⁻⁵ However, the mechanisms of myofibroblast differentiation and ECM deposition in COPD remain poorly understood but involve aberrant inflammation and dysregulated cellular responses to CS exposure.^{6,7}

Let-7, one of the first-discovered microRNAs, has an important role in respiratory diseases, including cancer, fibrosis and asthma.⁸⁻¹⁰ MicroRNAs are short non-coding RNAs that bind to the 3' untranslated regions of messenger RNAs (mRNAs),¹¹ and involved in many biological processes.¹²⁻¹⁴ Down-regulation of let-7 is common in many cancer types, and its replacement for normal expression has been found to prevent cancer growth.¹⁵ Lack of let-7 leads to a gain of profibrotic phenotype in lung epithelial cells in vitro and changes consistent with early fibrotic changes in vivo.¹⁶ It is reported that let-7 microRNAs represent a major regulatory mechanism for modulating IL-13 secretion in IL-13-producing cell types and, thereby, Th2 inflammation in asthma.¹⁷ Let-7 family, along with their potential target genes, functions as potential key microRNA-mRNAs in regulating chronic mucus hypersecretion in COPD.¹⁸ Although let-7 is involved in the pathogenic processes of COPD, its role in mediating the dysfunction of myofibroblast differentiation and ECM deposition in the context of CS exposure is undefined.

IL-6 is a multifunctional cytokine that has a role in fibrosis. It is demonstrated that overexpression of IL-6 is sufficient to induce myofibroblastic proliferation, differentiation and fibrosis, probably via increased TGF- β 1-mediated MMP2/MMP3 signalling in ischaemic myocardial remodelling.¹⁹ In addition, studies show that IL-6 has a central role in cardiomyocyte hypertrophy and myocardial fibrosis that is mediated by activating the MAPK and CaMKII-STAT3 pathways and that neutralizing IL-6 prevented cardiac fibroblasts activation.²⁰ IL-6-deficient mice display significantly delayed cutaneous wound closure, and expression of α -SMA mRNA was found to be increased in wounds of IL-6-deficient mice.²¹ In the Spyros study, high level of IL-6 characterizes early-on idiopathic pulmonary fibrosis acute exacerbations (IPF-AEs), and an increase in the level of IL-6 associates with worse outcome in all patients.²² In vitro activation of IL-6 trans-signalling enhanced fibroblast proliferation and extracellular matrix protein production, effects relevant in the progression of pulmonary fibrosis.²³ IL-6 is considered a cardinal stimulator of the production of most acute-phase

proteins in response to varied stimuli.²⁴ IL-6 can be produced by several cell types, and HBE cells secrete much more IL-6 by the stimulation of CSE.^{25,26}

Here, we hypothesized that down-regulation of let-7 in bronchial epithelial cells disturbs the communication between bronchial epithelial cells and fibroblasts via the regulation of IL-6 and mediates myofibroblast differentiation and ECM deposition. Therefore, we comprehensively investigated the expression variation of let-7 family in COPD and the effect of IL-6 on myofibroblast differentiation and ECM deposition. Better understanding of the molecular mechanisms underlying myofibroblast differentiation and ECM deposition is, thus, relevant to the prevention regimens targeting COPD pathogenesis. It is of great significance to seek new therapeutic targets for COPD.

2 | MATERIALS AND METHODS

2.1 | Cell culture and treatment

Study subjects were patients scheduled for bronchoscopies in WuXi People's Hospital. After using 20 mL saline to lavage the second and third generation of bronchi, five consecutive brushing samples were collected from the bronchial mucosa. Cells were harvested into a tube containing 5 mL RPMI1640 (HyClone, USA) after each brushing. About 25 mL liquid was filtered with a cell strainer (Falcon, USA). After centrifuging at 1000 rpm for 5 min, the cell pellet was resuspended in BEGM (Lonza, USA). Primary bronchial epithelial cells were harvested after seven to 25 days (Figure S2).

HBE cells, an SV40-transformed, normal HBE cell line and MRC-5 cells were all obtained from Chi Scientific (Jiangsu, China). HBE cells were cultured in a humidified incubator containing 95% air and 5% CO₂ at 37°C in Dulbecco's modified Eagle's medium (DMEM), supplemented with 10% foetal bovine serum (FBS) (Biological Industries, Italy), 100 U/mL penicillin and 100 μ g/mL streptomycin (Thermo Fisher Scientific, USA). MRC-5 cells were cultured in a humidified incubator containing 95% air and 5% CO₂ at 37°C in minimum essential medium (MEM) Eagle supplemented with 10% FBS (Biological Industries, Italy) and nonessential amino acids (NEAA) (Gibco, USA). MRC-5 cells were used for experiments at the third to fifth passage. After reaching 70% to 80% confluence, the cells were seeded into cell culture plates using 0.25% trypsin (Gibco, CA, USA) and exposed to 5% CSE for 24 h.

In a co-culture model, normal, CSE-treated or let-7 mimics transfected HBE cells were seeded onto 6-well plates, with MRC-5 cells co-cultured on 0.4 μ m pore, 24-mm-diameter insert (#3412, Corning, USA). HBE cells were treated with IL-6 antibody (MAB 206, R & D system, USA) and 5% CSE before they were placed in co-culture with MRC-5 cells. HBE cells

were transfected with let-7 mimic for 48 h and treated with 5% CSE before they were placed in co-culture with MRC-5 cells.

2.2 | Human sample collection

Peripheral lung tissues were collected from COPD patients undergoing lung transplantation and patients scheduled for pulmonary lobectomy in Wuxi People's Hospital. All peripheral lung tissue donations were voluntary, with full written informed consents, and in compliance with the Declaration of Istanbul. Peripheral lung tissues were placed into five to six cryogenic vials, frozen quickly in liquid nitrogen and then stored at -80°C for later use.

Serum samples were obtained from COPD patients who were admitted to the Wuxi People's Hospital between 2019 and 2020. Control serum samples were obtained from healthy volunteers who came to the hospital for a medical examination. All serum sample donations were voluntary, with full written informed consents, and in compliance with the Declaration of Istanbul. All serum samples were stored at -80°C .

All COPD patients met the diagnosis of GOLD 2019. Lung function and medical history of subjects participating in the study are reported in Table 2, Table 3 and Table 4. As shown in the tables, median age and sex ratio were similar in nonsmokers (Control-NS), smokers (Control-S) and COPD subjects.

This study was approved by the Ethics Committee of Wuxi People's Hospital Affiliated to Nanjing Medical University. This study was conducted in accordance with the Declaration of Helsinki, and written informed consents were received

from all participants. Reporting of the study conforms to the broad EQUATOR guidelines (Simera et al January 2010 issue of EJCI).

2.3 | Preparation of CSE

CSE was prepared as previously reported with some modifications.^{27,28} Briefly, the smoke of a Da Qian Men (10 mg tar and 0.8 mg nicotine/cigarette, Shanghai, China) was bubbled through 10 mL of serum-free DMEM. The resulting suspension was adjusted to pH 7.4 and then filtered through a 0.22- μm pore filter (Merck Millipore, USA) to remove bacteria and large particles. The CSE was standardized by monitoring the absorbance at 320 nm and defined as 100% CSE. The CSE was diluted to the desired concentration with medium and used in experiments within 30 min.

2.4 | RNA extraction and real-time PCR

Total RNA was isolated by use of RNAiso Plus (9108/9109, Takara, Japan). For microRNA and mRNA detection, total RNA (1 μg) was transcribed into cDNA by use of PrimeScriptTM RT reagent kit with gDNA eraser (RR047A, Takara, Japan) according to the manufacturer's recommendations. The sequences of mature microRNAs were from miRDB database. All of the primers were synthesized by Sangon Biotech (Shanghai, China). Primers used are listed in Table 1. The RT-PCR assay was performed with TB GreenTM Premix Ex TaqTM II (RR820A, Takara,

TABLE 1 Primers used in the study

Genes	Sequence (5' to 3')
Let-7a-RT	CTCAACTGGTGTCTGGAGTCGGCAATTCAGTTGAGAACTATAC
Let-7a-F	CCAGCTGGGTGAGGTAGTAGGTTGT
Let-7a-R	CTGGTGTCTGGAGTCGGCAATT
Let-7c-RT	GTCGTATCCAGTGCAGGGTCCGAGGTATTCGCACTGGATACGACAACCAT
Let-7c-F	CCAGCTGGGTGAGGTAGTAGGTTGT
Let-7c-R	TCCAGTGCAGGGTCCGAGGTA
Let-7d-RT	CTCAACTGGTGTCTGGAGTCGGCAATTCAGTTGAGAACTATGC
Let-7d-F	CCAGCTGGGAGAGGTAGTAGGTTGC
Let-7d-R	CTGGTGTCTGGAGTCGGCAATT
U6-RT	GTCGTATCCAGTGCAGGGTCCGAGGTATTCGCACTGGATACGACAAAATA
U6-F	AGAGAAGATTAGCATGGCCCCTG
U6-R	ATCCAGTGCAGGGTCCGAGG
H-IL-6-F	CACTGGTCTTTTGGAGTTTGAG
H-IL-6-R	GGACTTTTGTACTCATCTGCAC
M-IL-6-F	CTCCCAACAGACCTGTCTATAC
M-IL-6-R	CCATTGCACAACCTCTTTTCTCA

Abbreviations: F, forward; R, reverse; RT, reverse transcription.

Japan) and ABI 9600 real-time PCR detection system (Applied Biosystems). U6 was used as internal control for microRNA. GAPDH served as internal control for mRNA. Fold changes in expression of each gene were calculated by a comparative threshold cycle (Ct) method using the formula $2^{-(\Delta\Delta Ct)}$. Three independent experiments were carried out.

2.5 | Western blot

Total lysates were prepared according to the manufacturer's recommendations (Beyotime Institute of Biotechnology, Shanghai, China). Protein concentrations were measured with the BCA protein assay according to the manufacturer's manual (Beyotime Institute of Biotechnology, Shanghai, China). Equal amounts (30 μ g) of protein were separated by 10% sodium dodecyl sulphate–polyacrylamide gel electrophoresis and were transferred to polyvinylidene fluoride (PVDF) membranes (Millipore, Billerica, MA). Membranes were incubated overnight at 4°C with mouse anti-GAPDH antibody (ab8245, Abcam), mouse anti- β -actin antibody (66009-1-Ig, Proteintech), rabbit anti-E-cadherin antibody (#3195, Cell Signaling Technology), rabbit anti-alpha smooth muscle actin antibody (α -SMA) (ab32575, Abcam) and rabbit anti-collagen I antibody (ab138492, Abcam). After several washing steps, the membrane was incubated with secondary horseradish peroxidase (HRP)-conjugated antibody at room temperature for one hour. Detection was performed with the Immobilon ECL system (Millipore, S.p.A., Italy). Three independent experiments were carried out. The densitometric analyses of the bands were performed with ImageJ software.

2.6 | ELISA assay

Cell supernatant was centrifuged at 3000 rpm for 5 min, and then, the supernatant was collected and stored at -80°C until analyses. IL-6 protein level was evaluated with human IL-6 ELISA kit (R & D Systems, USA) according to the manufacturer's instructions.

2.7 | Transfection of let-7c mimics

Let-7c mimics and negative control (NC) mimics were purchased from Jikai Gene (Shanghai, China). The cells were seeded in a six-well plate at a density of 0.5×10^6 per well. After the cells reached 70% confluence, the transfection experiment was conducted using Lipofectamine 2000 reagent (Thermo Fisher Scientific, USA), according to the manufacturer's protocol. For the increases in let-7c mimics of HBE cells, the cells were transfected with 2 μ g let-7c mimics and

NC mimics in each well, respectively. After transfection for 48 h, the cells were exposed to 5% CSE for 24 h, and then, all group cells were harvested for the subsequent assays.

2.8 | Luciferase reporter assay

Luciferase activity was assessed as previously reported. To investigate the effect of let-7c on the 3'UTR of IL-6, which was predicted to combine with the let-7c region (*GAGGUA*), IL-6 was inserted into the XbaI/XbaI sites of the GV272 (Figure S1). These were named IL-6-wt (TACCTC) and IL-6-mut (ATGGAG), respectively (Designed by Jikai Gene, Shanghai, China). Confluent (70% to 80%) 293T cells were co-transfected with wild-type or mutant IL-6 3'UTR luciferase mimics and let-7c mimics or NC mimics using Lipofectamine 2000 (Thermo Fisher Scientific, USA). After 48 h of transfection, the cells were harvested for detection using the Dual-Luciferase Reporter assay system (Promega, USA) with an Infinite 200 PRO multimode microplate reader (Tecan Group, Ltd., Switzerland). Renilla luciferase activities were used to normalize the transfection efficiency.

2.9 | Establishment of murine COPD model

Male C57BL6J mice at 6 to 8 weeks of age were purchased from Changzhou Kawensi Experimental Animal Co., Ltd. (China) and housed in animal facilities at Wuxi People's Hospital, Jiangsu Province. Animals were treated humanely and with regard for alleviation of suffering according to a protocol approved by Wuxi People's Hospital, Jiangsu Province Institutional Animal Care and Use Committee, in compliance with law of Jiangsu Province on the administration of experimental animals. Mice were exposed to smoke from Da Qian Men (10 mg tar and 0.8 mg nicotine/cigarette, Shanghai, China) as described previously. Briefly, mice were exposed to CS in a whole-body exposure system in tempered glass box for 2 h twice a day, 4 h apart, 7 days a week for a total of 12 weeks. Age-matched mice kept in a similar environment without exposure to CS served as controls.

2.10 | Lung function measurement

Lung function of the mice was measured in Jiangsu Provincial Center for Disease Control and Prevention by use of whole-body plethysmography (Buxco Electronics, Ltd., USA) as previously reported. Briefly, mice were placed unrestrained in a chamber connecting a sensitive pressure transducer to measure pressure changes inside the chamber. Enhanced pause (Penh) was recorded using FinePointe software (Buxco Electronics, Ltd., USA) when the mice were quiet. Penh

generally reflects pulmonary resistance in all recorded respiratory parameters. Values were averaged and expressed as absolute Penh values.

2.11 | Collection of bronchoalveolar lavage fluid (BALF)

In anaesthetized mice, the skin and muscles of the anterior neck were incised to expose the trachea. The puncture needle was fixed in the trachea at an angle of 30 degrees. The right mainstem bronchus was clamped with an arterial clip, and then a syringe was attached to the arterial puncture needle. Then 0.4 mL of ice-cold, sterile phosphate-buffered saline solution was injected into the left lung and slowly aspirated back. The recovery rate was not less than 90%.

2.12 | Histopathology and Masson's staining

Mouse middle lobe of right lung and human lung tissues were fixed with 4% neutral paraformaldehyde for 24h. Tissues were embedded in paraffin, then sectioned (4 μ m). For the detection of collagen deposition, the sample slides were stained with trichrome stain (Masson's) kits (G1345, Solarbio, China) according to the manufacturer's instructions. After staining, the slides were examined under a light microscope by a photograph documentation facility (Olympus, Tokyo, Japan). Collagen content was determined by the ratio of collagen surface area (blue) to total surface area (red) with ImageJ software.

2.13 | Statistical analysis

All the relevant data are expressed as mean \pm SD of three independent experiments. Differences between mean values of normally distributed data were analysed using one-way ANOVA (Dunnett's *t* test), two-tailed Student's *t* test and Kruskal-Wallis test. The statistical analyses were conducted using SPSS 20 software, and values of $P < .05$ were considered to be statistically significant.

3 | RESULTS

3.1 | Airway remodelling in COPD patients

Masson's staining evidenced more collagen deposition in COPD patients compared with that in nonsmokers and smokers without COPD (Figure 1A,B). E-cadherin was down-regulated and α -SMA was up-regulated in the peripheral lung tissue of COPD patients (Figure 1C,D).

3.2 | Decreased let-7 and increased IL-6 in COPD patients

To determine whether let-7 is a mediator for COPD, the let-7 expression was explored in peripheral lung tissues (Table 2 and Table S1), primary bronchial epithelial cells (Table 3 and Table S2) and serum (Table 4 and Table S3). Let-7 in COPD patients' lung tissues was lower than that in nonsmokers and

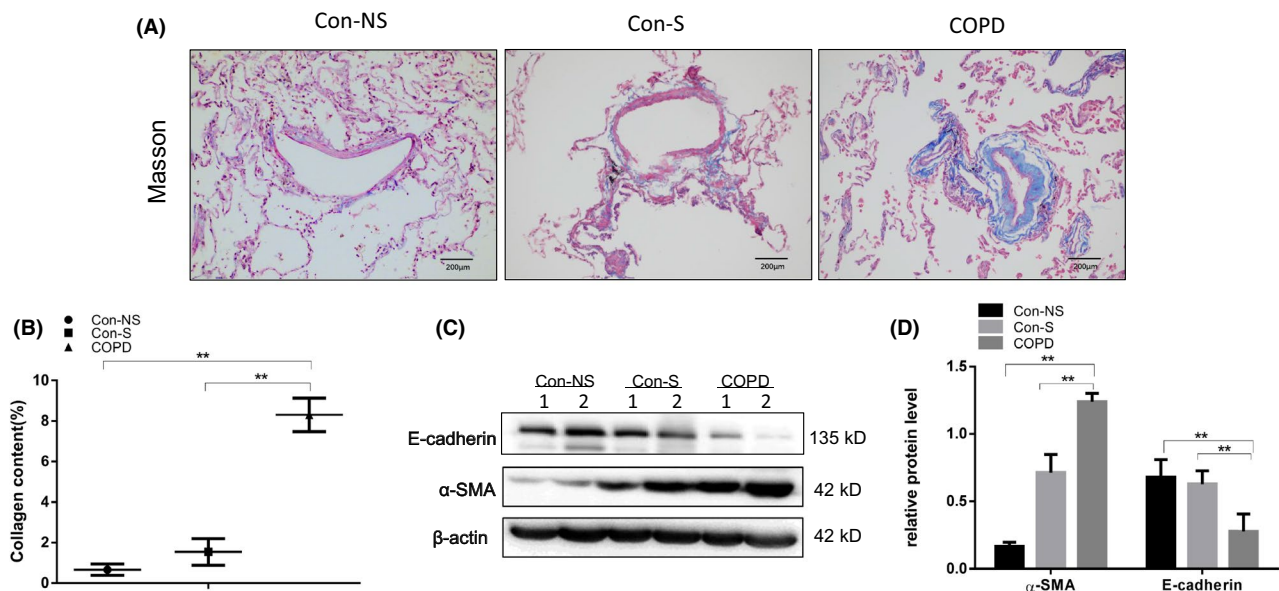


FIGURE 1 Collagen, α -SMA and E-cadherin in COPD patients. Con-NS, nonsmokers without COPD; Con-S, smokers without COPD; COPD, COPD patients. (A) Lung morphology was assessed by Masson's staining of lung sections. Scale bars, 200 μ m. Collagen: blue; nuclei: black; cytoplasm/epithelial: red. (B) Quantification of Masson's staining for collagen content from nonsmokers, smokers and COPD patients. (C) Western blots. (D) Relative protein levels of α -SMA and E-cadherin in lung were determined. Data are mean \pm SD (n = 3)

	Nonsmoker without COPD(control-NS)	Smokers without COPD(control-S)	COPD patients
Number	8	6	11
Male, n (%)	4 (50.0%)	4 (63.67%)	7 (63.64%)
Age (years)	56.50 ± 13.15	62.17 ± 2.4	61.64 ± 4.37
Smoking (pack-years)	0	43.33 ± 9.43	32.05 ± 21.18
FEV1% pred	95.06 ± 8.49	92.53 ± 4.75	27.27 ± 10.57
FEV1/FVC(%)	88.52 ± 4.39	79.68 ± 2.16	39.36 ± 6.44

Abbreviations: COPD, chronic obstructive pulmonary disease; pack-year, number of cigarettes smoked per day/20 (pack) × duration of smoking (year); FEV1, forced expiratory volume in one second; FVC, forced vital capacity; FEV1% pred, forced expiratory volume in one second per cent predicted. Data presented as mean ± SD.

	Nonsmokers without COPD (control-NS)	Smokers without COPD (control-S)	COPD patients
Number	6	6	6
Male, n (%)	4 (63.67%)	4 (63.67%)	4 (63.67%)
Age (years)	46.67 ± 7.37	56.33 ± 7.54	59.0 ± 8.64
Smoking(pack-years)	0	20.0 ± 8.66	35.0 ± 28.14
FEV1% pred	95.17 ± 13.8	86.76 ± 4.79	62.43 ± 15.27
FEV1/FVC(%)	88.67 ± 4.88	78.66 ± 4.48	57.68 ± 4.93

Abbreviations: COPD, chronic obstructive pulmonary disease; pack-year, number of cigarettes smoked per day/20 (pack) × duration of smoking (year); FEV1, forced expiratory volume in one second; FVC, forced vital capacity; FEV1% pred, forced expiratory volume in one second per cent predicted. Data presented as mean ± SD.

TABLE 4 Characteristics of bronchial epithelial cells in the study

	Control	COPD patients
Number	6	12
Male, n (%)	4 (63.67%)	8 (63.67%)
Age (years)	50.67 ± 6.07	65.67 ± 11.03
Smoking(pack-years)	NA	24.83 ± 23.33
FEV1% pred	NA	42.13 ± 16.33
FEV1/FVC(%)	< 70	51.1 ± 13.45

Abbreviations: COPD, chronic obstructive pulmonary disease; pack-year, number of cigarettes smoked per day/20 (pack) × duration of smoking (year); FEV1, forced expiratory volume in one second; FVC, forced vital capacity; FEV1% pred, forced expiratory volume in one second per cent predicted. NA, not acquired. Data presented as mean ± SD.

smokers (Figure 2A). As the peripheral lung contains many different types of cells, we examined the expression of let-7 in primary bronchial epithelial cells isolated from subjects with or without COPD. As shown in Figure 2B, let-7 in the primary cells was decreased compared with that in nonsmokers and smokers. What's more, Let-7 in COPD patients' serum was lower than that in control group (Figure 2C). We

TABLE 2 Characteristics of peripheral lung tissues in the study

TABLE 3 Characteristics of bronchial epithelial cells in the study

also detected IL-6 mRNA expression in peripheral lung tissues and primary bronchial epithelial cells. IL-6 mRNA in COPD patients' lung tissues and primary bronchial epithelial cells was higher than both that in nonsmokers and smokers (Figure 2D,E). IL-6 in the cell supernatant from primary epithelial cells was increased compared with that in nonsmokers and smokers (Figure 2F).

3.3 | Increased inflammation cells and airway remodelling in CS-exposed mice

After 12 weeks' exposure to CS, the mice developed COPD, showing inflammation and airway remodelling. Penh increased in CS-exposed mice compared to that in controls (Figure 3A). An increase in total cell number in the BALF was detected in mice exposed to CS compared with that in controls (Figure 3B). Furthermore, the CS-exposed mice developed an airway remodelling phenotype, showing airway thickening and collagen deposition. Masson's staining showed more collagen deposition in CS-exposed mice (Figure 3C,D). Western blot also revealed that E-cadherin was decreased and α -SMA was increased in lung tissue of CS-exposed mice (Figure 3E,F).

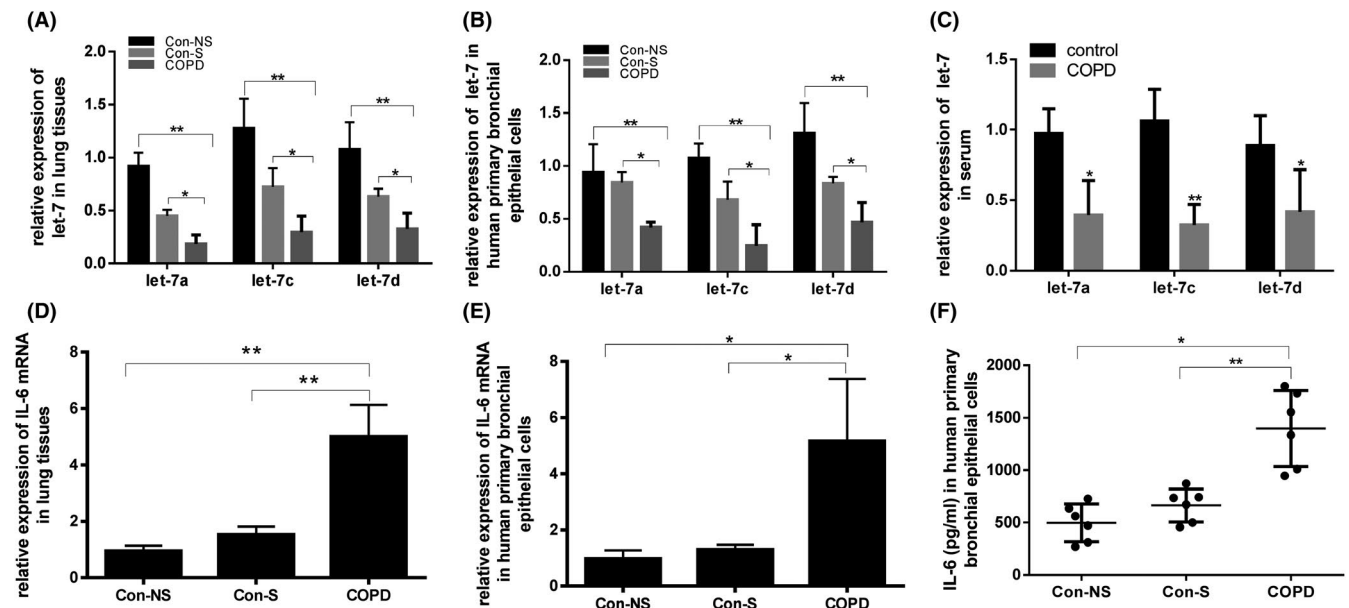


FIGURE 2 Expression of let-7 and IL-6 in COPD patients. Con-NS, nonsmokers without COPD; Con-S, smokers without COPD; COPD, COPD patients. (A) Levels of let-7 in peripheral lung tissues of Con-NS (n = 8), Con-S (n = 6), and COPD (n = 11) were determined by RT-PCR. (B) Levels of let-7 in human primary bronchial epithelial cells (n = 6) were determined by RT-PCR. (C) Levels of let-7 in serum of control group (n = 6) and COPD patients (n = 12) were determined by RT-PCR. (D) Relative expression of IL-6 mRNA in peripheral lung tissues was detected by RT-PCR. (E) Relative expression of IL-6 mRNA in human primary bronchial epithelial cells (n = 6) was detected by RT-PCR. (F) IL-6 derived from human primary bronchial epithelial cells (n = 6) was explored by ELISA. Data are mean \pm SD

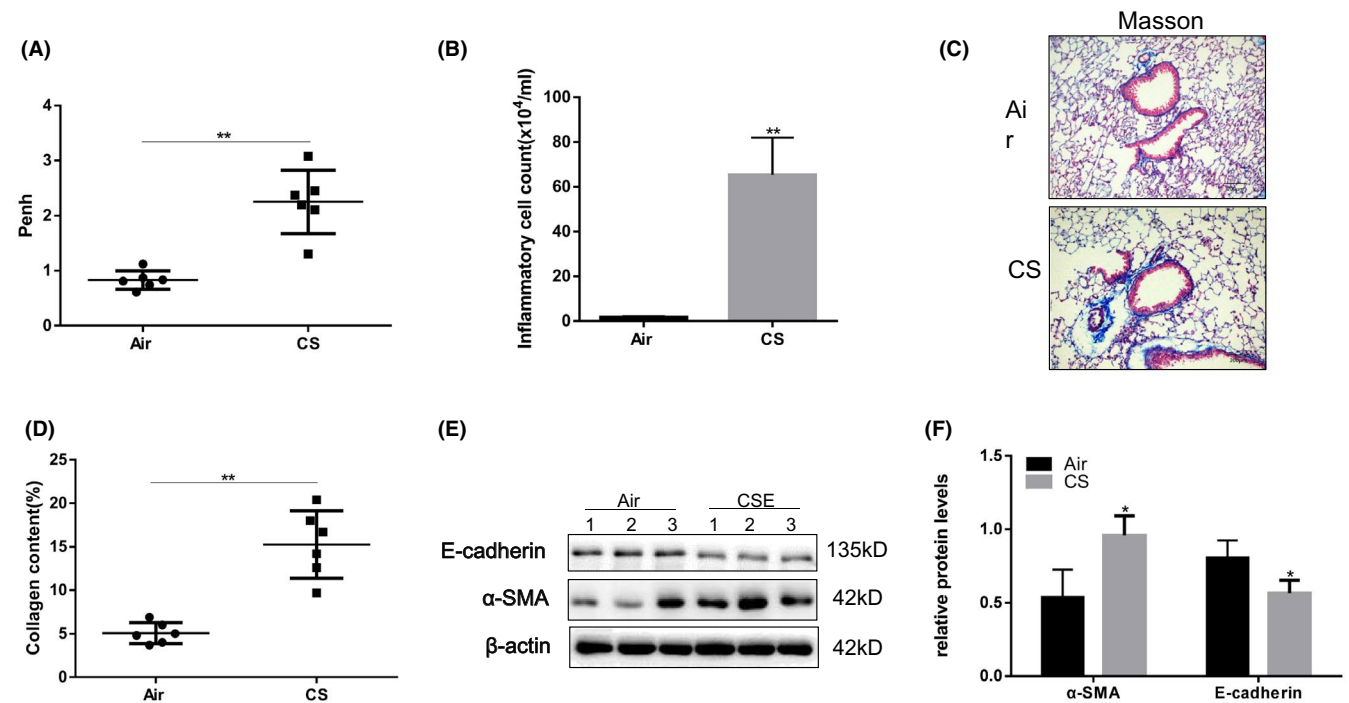


FIGURE 3 CS-exposed mice. Male C57BL6J mice at 6-8 weeks of age were exposed to CS for 12 weeks. Pulmonary function was represented as Penh (A) in air-exposed mice and CS-exposed mice. (B) Total inflammatory cell count of BALF from air-exposed mice and CS-exposed mice. (C) Lung morphology was assessed by Masson's staining of lung sections. Collagen: blue; nuclei: black; cytoplasm/epithelial: red. Scale bars, 200 μ m. (D) Quantification of Masson's staining for collagen content. (E) Western blots were performed, and (F) relative protein levels of α -SMA and E-cadherin in lung were determined. All data are shown as mean \pm SD (n = 6)

3.4 | Decreased let-7 and increased IL-6 in CS-exposed mice and CSE-treated HBE cells

There were lower expressions of let-7 in the peripheral lung tissue of CS-exposed mice compared to that in air groups (Figure 4A and Table S4). Significant differences in the expressions of let-7a, let-7c and let-7d were observed in CS-exposed mice compared to controls. We detected IL-6 mRNA in CS-exposed mice higher than in control groups (Figure 4B). We confirmed that let-7 expression correlated with CSE concentration. The 5% CSE-treated HBE cells showed lower expression in let-7a, let-7c and let-7d than the 2% CSE-treated HBE cells (Figure 4C and Table S5). IL-6 mRNA levels were obviously increased at 2% and 5% CSE concentrations compared with that in control groups (Figure 4D). Secreted IL-6 in cell supernatant was increased at 24 h, 48 h and 72 h after CSE exposure (Figure 4E).

3.5 | Let-7 down-regulated IL-6 in CSE-treated HBE cells

Through the analysis of three different databases (TargetScan, miRDB and miRBase), we found that all the members of let-7 family (GAGGUA) had the same potential binding site

to the 3'UTR of IL-6 (TACCTC). Among 12 microRNAs of let-7 family, RT-PCR results confirmed let-7a, let-7c and let-7d were significantly down-regulated in both peripheral lung tissue of COPD patients and CSE-treated HBE cells in comparison with controls. By consulting related articles, we chose let-7c for subsequent experiments. Luciferase reporter assays were conducted using mimics of wild-type and mutant IL-6 that contained let-7c binding sites in 3'UTR (Figure 5C). Following co-transfected mimics of wild-type IL-6 and let-7c in 293T cells, there was low luciferase activity. However, co-transfected mimics of let-7c with mutated IL-6 resulted in no appreciable change in luciferase activity (Figure 5D,E). RT-PCR and ELISA analysis showed that IL-6 was decreased in let-7c transfected HBE cells (Figure 5A,B).

3.6 | Let-7 promoted myofibroblast differentiation of human lung fibroblasts by regulating IL-6 secretion

Collagen I and α -SMA were up-regulated in MRC-5 cells co-cultured with CSE-treated HBE cells (Figure 6A,B). Additionally, antibody against IL-6 was added to the co-culture system, and protein levels in the MRC-5 cells were detected by western blot analysis. The neutralizing antibody

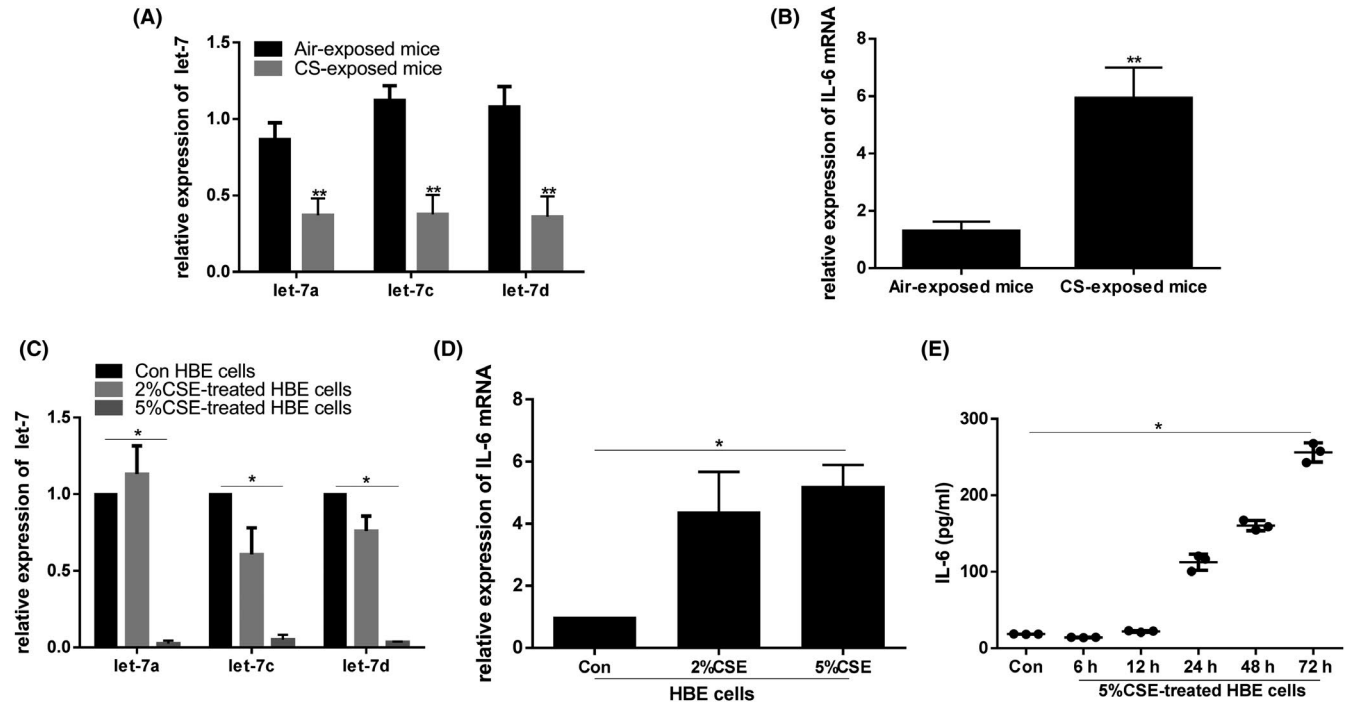


FIGURE 4 Expression of let-7 and IL-6 in CS-exposed mice and CSE-treated HBE cells. Con, control; 2% CSE, HBE cells treated with 2% CSE for 24 h; 5% CSE, HBE cells treated with 5% CSE for 24 h. (A) Levels of let-7 in CS-exposed mice compared with air-exposed mice were determined by RT-PCR. (B) Relative expression of IL-6 mRNA in lung tissue of CS-exposed mice and air-exposed mice revealed by RT-PCR. (C) Levels of let-7 in HBE cells treated with 2% CSE and 5% CSE detected by RT-PCR. (D) Relative expression of IL-6 mRNA in HBE cells by RT-PCR. (E) IL-6 derived from 5% CSE-treated HBE cells induced with different times was explored by ELISA. All data are shown as mean \pm SD (n = 6 in mice, n = 3 in HBE cells)

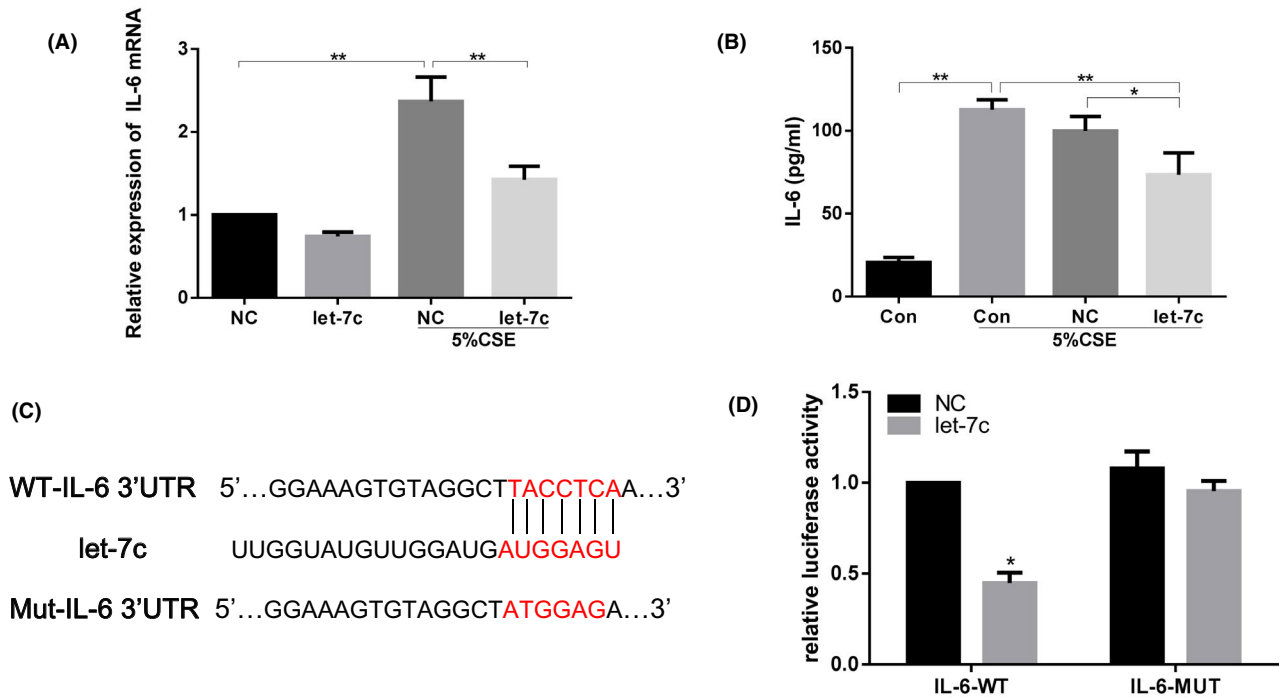


FIGURE 5 Let-7 can regulate IL-6 in HBE cells. NC, HBE cells treated with NC mimic for 48 h. Let-7c, HBE cells treated with let-7c mimic for 48 h. NC + 5% CSE, HBE cells treated with NC mimic for 48 h, then induced by 5% CSE for 24 h. Let-7c + 5% CSE, HBE cells treated with let-7c mimic for 48 h, then induced by 5% CSE for 24 h. (A) RT-PCR was performed to detect expression of IL-6 mRNA in HBE cells. (B) ELISA was performed to determine IL-6 secreted by HBE cells. (C) Schematic of let-7c putative target sites in the 3' UTR of IL-6 and sequences of mutant UTRs. (D) Luciferase reporter assay was performed after co-transfected with let-7c mimic or NC mimic and IL-6-wt mimic or IL-6-mut mimic. Data are mean \pm SD (n = 3)

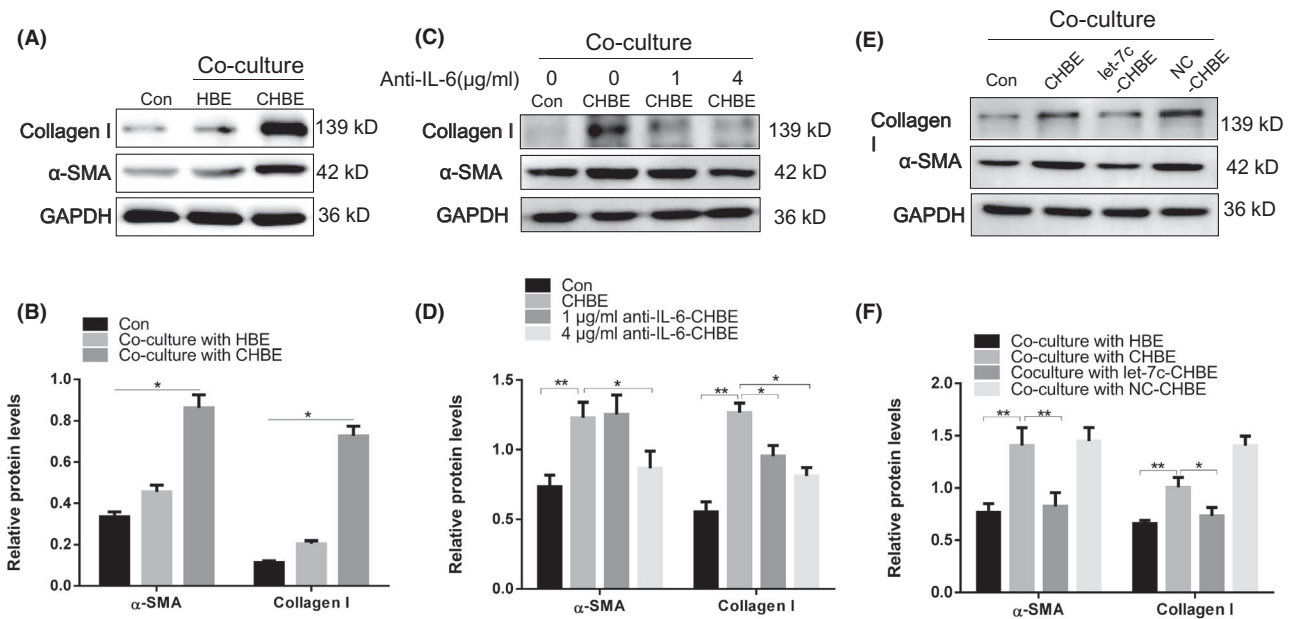


FIGURE 6 Let-7 in HBE cells can promote myfibroblast differentiation of MRC-5 cells. CHBE, HBE treated with 5% CSE; let-7c-CHBE, HBE cells transfected with let-7c mimic, then treated with 5% CSE; NC-CHBE, HBE cells transfected with NC mimic, then treated with 5% CSE. MRC-5 cells were co-cultured with HBE, CHBE, let-7c-CHBE and NC-CHBE. Densities of bands were quantified by ImageJ software. GAPDH levels, measured in parallel, served as controls. (A, B) MRC-5 cells were co-cultured with HBE, CHBE, and the levels of α -SMA and collagen I were determined using Western blot. (C, D) MRC-5 cells were co-cultured with HBE, CHBE. IL-6 (1 μ g/ml and 4 μ g/ml) antibodies were added and levels of α -SMA and collagen I were detected by Western blots. MRC-5 cells were co-cultured with CHBE, let-7c-CHBE, NC-CHBE. (E) Western blots were performed, and (F) protein levels of α -SMA and collagen I were determined. Data are mean \pm SD (n = 3)

decreased the expression of Collagen I and α -SMA in MRC-5 cells (Figure 6C,D). For validation, let-7c mimic was transfected in HBE cells. RT-PCR and ELISA analysis showed that IL-6 expression was decreased in let-7c mimic transfected HBE cells (Figure 5A,B). Western blotting revealed that, in the MRC-5 cells co-cultured with CHBE cells which were transfected with let-7c mimic, collagen I and α -SMA were decreased more than in CSE-treated HBE cells (Figure 6E,F).

4 | DISCUSSION

COPD is a worldwide public health challenge because of its high prevalence, disability and mortality.²⁹ Cigarette smoking is known to cause airway remodelling, leading to irreversible loss of lung function in COPD. The overly enhanced activity of myofibroblasts leads to airway fibrosis in general with aberrant ECM deposition and remodelling in COPD. Our study presented that IL-6 exerted a positive role in regulating the differentiation of fibroblasts to myofibroblasts in airway remodelling. We proposed that, as an underlying mechanism, down-regulation of let-7 induced by cigarette smoke played an important role in this process.

Airway remodelling in COPD involves mucous glandular metaplasia, myofibroblast proliferation and ECM deposition.³⁰ Remodelling of the airways contributes to progressive and largely irreversible airflow limitation.³¹ We did find airway remodelling in COPD patients and CS-exposed mice, manifesting as collagen deposition and epithelial-mesenchymal transition (EMT). These findings are in accordance with previous observations.^{32,33} During this process, myofibroblasts, which originate directly from lung bronchial fibroblasts, are involved in the formation of airway fibrosis.³⁴ The differentiation of fibroblasts to myofibroblasts not only contributes to fibrosis by releasing collagens, but also stimulates the epithelium to release more cytokines and inflammatory factors, which may form a vicious cycle for small airway narrowing and airflow obstruction.³⁵ Multiple observers have noted the presence of abnormal myofibroblast differentiation and ECM deposition in COPD, but the regulatory mechanisms have not been fully elucidated. In the present study, we found that CS-exposed mice not only showed airway remodelling phenotype, but also demonstrated increased inflammation. The total inflammatory cell count in BALF was increased. These findings suggest that inflammatory factors and inflammatory cells may play an important role in airway remodelling of COPD as well.

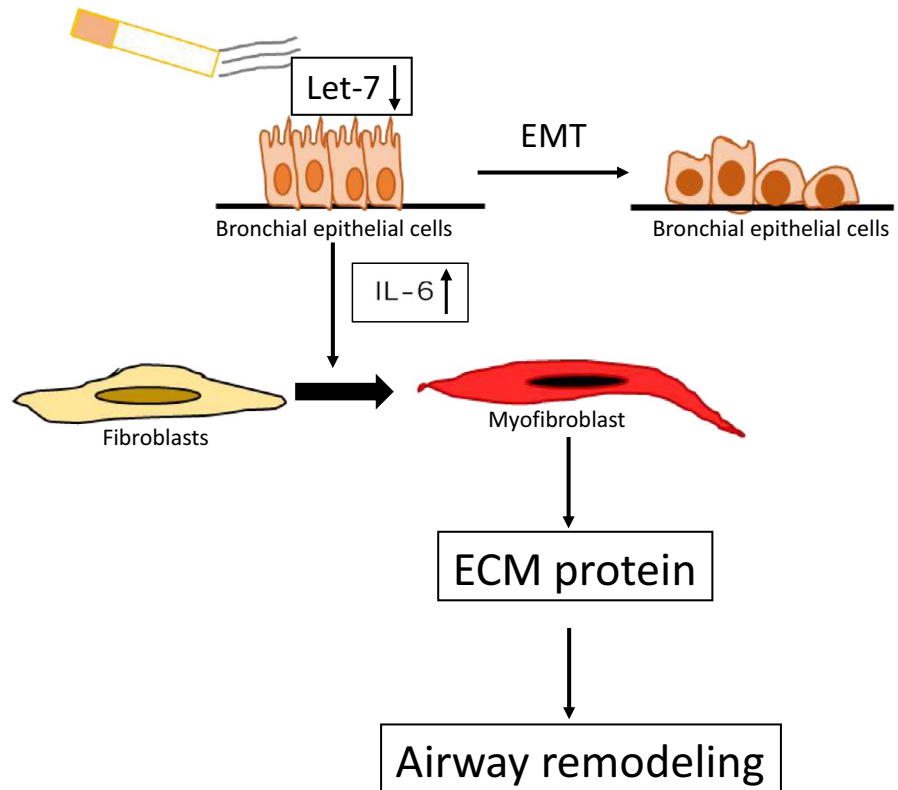
Inflammatory cells and structural cells involved in airway remodelling of COPD secrete a variety of proinflammatory mediators, including cytokines, chemokines and growth factors.³⁶ Among all the cytokines and chemokines, robustly increased IL-6 levels were found in BALF of COPD patients

and CS-exposed mice.^{37,38} Our study provided additional evidence that increased IL-6 was found in the cell supernatant of primary HBE cells of COPD patients as well as CSE-treated HBE cells, and IL-6 mRNA was increased in COPD patients, CS-exposed mice and CSE-treated HBE cells. IL-6 is involved in the pathogenesis of COPD, including features of chronic airway inflammation and airway remodelling, through a variety of signalling pathways.³⁹⁻⁴¹ Previous studies have reported that IL-6 is released from fibroblasts, endothelial cells and epithelial cells in COPD and could induce collagen synthesis.^{42,43} In order to confirm the effects of IL-6 on differentiation of bronchial fibroblasts to myofibroblasts, we co-cultured MRC-5 cells with CSE-treated HBE cells. The results revealed that CSE-treated HBE cells increased IL-6 secretion and promoted the differentiation of bronchial fibroblasts to myofibroblasts, manifested as up-regulation of α -SMA and collagen I in MRC-5 cells.

The mechanism of up-regulation of IL-6 in COPD is not completely understood. There is increasing evidence that let-7 directly targets IL-6 to suppress the IL-6 signalling pathway.^{44,45} Let-7, one of the first-discovered microRNA families, has 12 members (from let-7a to let-7i, and miR-98) and is located at eight different chromosomes.⁴⁶ In 2009, the possibility that a positive feedback loop of inflammation was formed by let-7, Lin28, NF- κ B, and IL-6 was first raised.⁴⁷ Recently, another report also showed that the down-regulation of let-7 enhanced the production of IL-6 by diesel exhaust particle exposure in mice.⁴⁸ Let-7 levels negatively correlated with aberrant inflammation. In our study, we validated IL-6 as a direct target of let-7 by using a luciferase reporter assay. Our results provide further evidence for the let-7/IL-6 signalling pathway. To further demonstrate the role of the let-7 in regulation of IL-6 expression, we treated HBE cells with the let-7 mimics and found IL-6 expression was significantly down-regulated. Let-7 mimic significantly inhibited the secretion of IL-6 as well as the differentiation of bronchial fibroblasts to myofibroblasts. These results suggest that IL-6 might act as a mediator of let-7 regulation of myofibroblast differentiation and ECM deposition.

Abnormal expression of let-7 family members is related to numerous diseases, including cancer and pulmonary fibrosis.^{8,49,50} Let-7 family members act as tumour suppressors because they not only are down-regulated in a variety of cancers, but also effect the expression of many oncogenes, including HMGA2 and RAS.⁵¹ It is reported that let-7d was significantly decreased in pulmonary fibrosis lungs, and this miRNA activity has also been reported to show a negative association with markers of fibrosis and fibroblast proliferation.⁵² A previous study, through gene set enrichment analysis and search tool for retrieving interacting genes/proteins (STRING) of bronchial biopsies from COPD patients reported that the let-7 family along with their potential target

FIGURE 7 Schematic representation of the potential role of let-7 in COPD. Let-7 is negatively regulated in bronchial epithelial cells and functions to secrete more IL-6, which normally promotes differentiation of bronchial fibroblasts to myofibroblasts. Myofibroblasts can promote ECM protein deposition, leading to airway remodelling in COPD



gene EDN1 may serve as potential key microRNA-mRNA for chronic mucus hypersecretion in COPD. Our results showed that let-7a, let-7c and let-7d were down-regulated in COPD patients. This result is in agreement with and extends the findings from that recent report.⁵³ Additionally, in this present work, we analysed the expression of let-7 in CS-exposed mice. Compared to air-exposed mice, CS-exposed mice that developed airway remodelling phenotype showed lower levels of let-7a, let-7c and let-7d. Furthermore, we confirmed that let-7 expression was decreased in CSE-treated HBE cells. These studies established the important function of let-7 in COPD.

Our study has some limitations. First, IL-6 protein levels were not studied in CS-exposed mice due to the lack of material. Additionally, the role of let-7 and its regulation of IL-6 was not investigated with in vivo models. Follow-up studies using in vivo models are encouraged to provide further mechanistic insights.

In conclusion, our results reveal that let-7a, let-7c and let-7d are involved in airway remodelling in COPD. IL-6, as the key mediator, participates in the crosstalk between bronchial epithelial cells and fibroblast cells. For bronchial epithelial cells, cigarette smoke exposure induces the decrease of let-7, which up-regulates the secretion of IL-6. In bronchial fibroblast cells, IL-6 elevates the expression of α -SMA and collagen I, inducing the differentiation of fibroblasts to myofibroblasts (Figure 7). These results indicate that let-7 has potential investigative value in the diagnosis and treatment of COPD.

ACKNOWLEDGEMENTS

We would like to express our sincere gratitude to Jingyu Chen for provision of transplantation specimens.

CONFLICT OF INTEREST

The authors declare that there are no conflicts of interest.

ORCID

Tingting Di  <https://orcid.org/0000-0003-0426-4700>

REFERENCES

1. Wang C, Xu J, Yang L, et al. Prevalence and risk factors of chronic obstructive pulmonary disease in China (the China Pulmonary Health [CPH] study): a national cross-sectional study. *Lancet*. 2018;391:1706-1717.
2. Wise RA, Chapman KR, Scirica BM, et al. Effect of acclidinium bromide on major cardiovascular events and exacerbations in high-risk patients with chronic obstructive pulmonary disease: The ASCENT-COPD randomized clinical trial. *JAMA*. 2019;321:1693-1701.
3. Barnes PJ. Small airway fibrosis in COPD. *Int J Biochem Cell Biol*. 2019;116:105598.
4. Ito JT, Lourenco JD, Righetti RF, Tiberio I, Prado CM, Lopes F. Extracellular matrix component remodeling in respiratory diseases: What has been found in clinical and experimental studies? *Cells*. 2019;8(4):342.
5. Yoshida T, Tuder RM. Pathobiology of cigarette smoke-induced chronic obstructive pulmonary disease. *PHYSIOL REV*. 2007;87:1047-1082.
6. Wang Y, Jia M, Yan X, et al. Increased neutrophil gelatinase-associated lipocalin (NGAL) promotes airway remodelling

- in chronic obstructive pulmonary disease. *Clin Sci (Lond)*. 2017;131:1147-1159.
7. Cloonan SM, Glass K, Laucho-Contreras ME, et al. Mitochondrial iron chelation ameliorates cigarette smoke-induced bronchitis and emphysema in mice. *Nat Med*. 2016;22:163-174.
 8. Elliot S, Periera-Simon S, Xia X, et al. MicroRNA let-7 downregulates ligand-independent estrogen receptor-mediated male-predominant pulmonary fibrosis. *Am J Respir Crit Care Med*. 2019;200:1246-1257.
 9. Trang P, Medina PP, Wiggins JF, et al. Regression of murine lung tumors by the let-7 microRNA. *Oncogene*. 2010;29:1580-1587.
 10. Chin LJ, Ratner E, Leng S, et al. A SNP in a let-7 microRNA complementary site in the KRAS 3' untranslated region increases non-small cell lung cancer risk. *Cancer Res*. 2008;68:8535-8540.
 11. Pourhanifeh MH, Mahjoubin-Tehran M, Karimzadeh MR, et al. Autophagy in cancers including brain tumors: role of MicroRNAs. *Cell Commun Signal*. 2020;18:88.
 12. Khani P, Nasri F, Khani Chamani F, et al. Genetic and epigenetic contribution to astrocytic gliomas pathogenesis. *J Neurochem*. 2019;148:188-203.
 13. Mirzaei H, Yazdi F, Salehi R, Mirzaei HR. SiRNA and epigenetic aberrations in ovarian cancer. *J Cancer Res Ther*. 2016;12:498-508.
 14. Hashemian SM, Pourhanifeh MH, Fadaei S, Velayati AA, Mirzaei H, Hamblin MR. Non-coding RNAs and Exosomes: Their Role in the Pathogenesis of Sepsis. *Mol Ther Nucleic Acids*. 2020;21:51-74.
 15. Barh D, Malhotra R, Ravi B, Sindhurani P. MicroRNA let-7: an emerging next-generation cancer therapeutic. *Curr Oncol*. 2010;17:70-80.
 16. Pandit KV, Milosevic J, Kaminski N. MicroRNAs in idiopathic pulmonary fibrosis. *Transl Res*. 2011;157:191-199.
 17. Kumar M, Ahmad T, Sharma A, et al. Let-7 microRNA-mediated regulation of IL-13 and allergic airway inflammation. *J Allergy Clin Immunol*. 2011;128:1077-1085.
 18. Tasena H, Faiz A, Timens W, et al. microRNA-mRNA regulatory networks underlying chronic mucus hypersecretion in COPD. *Eur Respir J*. 2018;52(3):1701556.
 19. Wang JH, Zhao L, Pan X, et al. Hypoxia-stimulated cardiac fibroblast production of IL-6 promotes myocardial fibrosis via the TGF-beta1 signaling pathway. *Lab Invest*. 2016;96:839-852.
 20. Kumar S, Wang G, Zheng NA, et al. HIMF (Hypoxia-Induced Mitogenic Factor)-IL (Interleukin)-6 Signaling Mediates Cardiomyocyte-Fibroblast Crosstalk to Promote Cardiac Hypertrophy and Fibrosis. *Hypertension*. 2019;73:1058-1070.
 21. Gallucci RM, Lee EG, Tomasek JJ. IL-6 modulates alpha-smooth muscle actin expression in dermal fibroblasts from IL-6-deficient mice. *J Invest Dermatol*. 2006;126:561-568.
 22. Papisir SA, Tomos IP, Karakatsani A, et al. High levels of IL-6 and IL-8 characterize early-on idiopathic pulmonary fibrosis acute exacerbations. *Cytokine*. 2018;102:168-172.
 23. Le TT, Karmouty-Quintana H, Melicoff E, et al. Blockade of IL-6 Trans signaling attenuates pulmonary fibrosis. *J Immunol*. 2014;193:3755-3768.
 24. Gabay C. Interleukin-6 and chronic inflammation. *Arthritis Res Ther*. 2006;8(Suppl 2):S3.
 25. Li D, Hu J, Wang T, et al. Silymarin attenuates cigarette smoke extract-induced inflammation via simultaneous inhibition of autophagy and ERK/p38 MAPK pathway in human bronchial epithelial cells. *Sci Rep*. 2016;6:37751.
 26. Cui W, Zhang Z, Zhang P, et al. Nrf2 attenuates inflammatory response in COPD/emphysema: Crosstalk with Wnt3a/beta-catenin and AMPK pathways. *J Cell Mol Med*. 2018;22:3514-3525.
 27. Li E, Xu Z, Liu F, et al. Continual exposure to cigarette smoke extracts induces tumor-like transformation of human nontumor bronchial epithelial cells in a microfluidic chip. *J Thorac Oncol*. 2014;9:1091-1100.
 28. Petecchia L, Sabatini F, Varesio L, et al. Bronchial airway epithelial cell damage following exposure to cigarette smoke includes disassembly of tight junction components mediated by the extracellular signal-regulated kinase 1/2 pathway. *Chest*. 2009;135:1502-1512.
 29. Chen L, Ge Q, Tjin G, et al. Effects of cigarette smoke extract on human airway smooth muscle cells in COPD. *Eur Respir J*. 2014;44:634-646.
 30. Chung KF. The role of airway smooth muscle in the pathogenesis of airway wall remodeling in chronic obstructive pulmonary disease. *Proc Am Thorac Soc*. 2005;2(347-54):371-372.
 31. O'Donnell DE, Parker CM. COPD exacerbations. 3: Pathophysiology. *Thorax*. 2006;61:354-361.
 32. Guan R, Wang J, Cai Z, et al. Hydrogen sulfide attenuates cigarette smoke-induced airway remodeling by upregulating SIRT1 signaling pathway. *Redox Biol*. 2019;28:101356.
 33. Lai T, Tian B, Cao C, et al. HDAC2 Suppresses IL17A-Mediated Airway Remodeling in Human and Experimental Modeling of COPD. *Chest*. 2018;153:863-875.
 34. Xu H, Ling M, Xue J, et al. Exosomal microRNA-21 derived from bronchial epithelial cells is involved in aberrant epithelium-fibroblast cross-talk in COPD induced by cigarette smoking. *Theranostics*. 2018;8:5419-5433.
 35. Sohal SS, Reid D, Soltani A, et al. Evaluation of epithelial mesenchymal transition in patients with chronic obstructive pulmonary disease. *Respir Res*. 2011;12:130.
 36. Barnes PJ. Inflammatory mechanisms in patients with chronic obstructive pulmonary disease. *J Allergy Clin Immunol*. 2016;138:16-27.
 37. Cheng Q, Fang L, Feng D, et al. Memantine ameliorates pulmonary inflammation in a mice model of COPD induced by cigarette smoke combined with LPS. *Biomed Pharmacother*. 2019;109:2005-2013.
 38. Lazar Z, Müllner N, Lucattelli M, et al. NTPDase1/CD39 and aberrant purinergic signalling in the pathogenesis of COPD. *Eur Respir J*. 2016;47:254-263.
 39. Comer DM, Kidney JC, Ennis M, Elborn JS. Airway epithelial cell apoptosis and inflammation in COPD, smokers and nonsmokers. *Eur Respir J*. 2013;41:1058-1067.
 40. Patel IS, Roberts NJ, Lloyd-Owen SJ, Sapsford RJ, Wedzicha JA. Airway epithelial inflammatory responses and clinical parameters in COPD. *Eur Respir J*. 2003;22:94-99.
 41. Saint-Criq V, Villeret B, Bastaert F, et al. Pseudomonas aeruginosa LasB protease impairs innate immunity in mice and humans by targeting a lung epithelial cystic fibrosis transmembrane regulator-IL-6-antimicrobial-repair pathway. *Thorax*. 2018;73:49-61.
 42. Mauw J, Denson JL, Bruning JC. Versatile functions for IL-6 in metabolism and cancer. *Trends Immunol*. 2015;36:92-101.
 43. Hunter CA, Jones SA. IL-6 as a keystone cytokine in health and disease. *Nat Immunol*. 2015;16:448-457.
 44. Wei YB, Liu JJ, Villaescusa JC, et al. Elevation of Il6 is associated with disturbed let-7 biogenesis in a genetic model of depression. *Transl Psychiatry*. 2016;6:e869.
 45. Schulte LN, Eulalio A, Mollenkopf HJ, Reinhardt R, Vogel J. Analysis of the host microRNA response to Salmonella uncovers the control of major cytokines by the let-7 family. *Embo J*. 2011;30:1977-1989.

46. Thornton JE, Gregory RI. How does Lin28 let-7 control development and disease? *Trends Cell Biol.* 2012;22:474-482.
47. Iliopoulos D, Hirsch HA, Struhl K. An epigenetic switch involving NF-kappaB, Lin28, Let-7 MicroRNA, and IL6 links inflammation to cell transformation. *Cell.* 2009;139:693-706.
48. Wang G, Zheng X, Tang J, et al. LIN28B/let-7 axis mediates pulmonary inflammatory response induced by diesel exhaust particle exposure in mice. *Toxicol Lett.* 2018;299:1-10.
49. Adams CM, Eischen CM. Histone deacetylase inhibition reveals a tumor-suppressive function of MYC-regulated miRNA in breast and lung carcinoma. *Cell Death Differ.* 2016;23:1312-1321.
50. Zhao B, Han H, Chen J, et al. MicroRNA let-7c inhibits migration and invasion of human non-small cell lung cancer by targeting ITGB3 and MAP4K3. *Cancer Lett.* 2014;342:43-51.
51. Johnson SM, Grosshans H, Shingara J, et al. RAS is regulated by the let-7 microRNA family. *Cell.* 2005;120:635-647.
52. Rezaei S, Mahjoubin-Tehran M, Aghaee-Bakhtiari SH, et al. Autophagy-related MicroRNAs in chronic lung diseases and lung cancer. *Crit Rev Oncol Hematol.* 2020;153:103063.
53. Qian Y, Mao ZD, Shi YJ, Liu ZG, Cao Q, Zhang Q. Comprehensive Analysis of miRNA-mRNA-lncRNA Networks in Non-Smoking and Smoking Patients with Chronic Obstructive Pulmonary Disease. *Cell Physiol Biochem.* 2018;50:1140-1153.

SUPPORTING INFORMATION

Additional supporting information may be found online in the Supporting Information section.

How to cite this article: Di T, Yang Y, Fu C, et al. Let-7 mediated airway remodeling in chronic obstructive pulmonary disease via the regulation of IL-6. *Eur J Clin Invest.* 2021;51:e13425. <https://doi.org/10.1111/eci.13425>